NOTES AND CORRESPONDENCE

An Interactive Nesting Algorithm for Stretched Grids and Variable Nesting Ratios

ROBERT L. WALKO, CRAIG J. TREMBACK, ROGER A. PIELKE, AND WILLIAM R. COTTON

Department of Atmospheric Science, Colorado State University, Fort Collins, Colorado

12 November 1993 and 1 June 1994

ABSTRACT

An existing two-way interactive grid-nesting technique is generalized to accommodate stretched grids and a spatially variable grid-nesting ratio. The new scheme applies the same reversibility constraint and possesses the same scalar and momentum conservation properties as its predecessor. The scheme can be applied in any coordinate direction but was motivated primarily by the common use of vertical grid stretching. The scheme is successfully tested in a simulation of a collapsing cold pool.

1. Introduction

This note presents a generalization of the grid-nesting scheme described in Clark and Farley (1984) and Clark and Hall (1991) (hereafter CFCH) in order to allow the scheme to be used with nonuniform grid spacing. The original CFCH scheme has been used for several years in the Regional Atmospheric Modeling System (RAMS) developed at Colorado State University for a wide variety of applications. While the CFCH scheme has performed quite successfully, the motivation to generalize it arose for two main reasons. First, RAMS usually employs a stretched grid in the vertical to achieve greater vertical resolution near the ground than at the higher model levels. If vertical nesting is to be used on a stretched grid to provide even greater vertical resolution on a nested grid (NG) relative to its parent grid (PG), the assumptions of constant mesh spacing made in CFCH need to be relaxed. Second, some model applications have required high vertical resolution only near the ground on an NG, for example, in simulating nocturnal drainage flows in a local mountain–valley system, while permitting coarser vertical resolution on the entire PG and at higher levels in the NG. Thus, we have included in the generalized nesting scheme the ability for a vertical nesting ratio to vary with height. Even with constant vertical spacing on the PG, this involves a variable spacing on the NG. While both these requirements for the generalized algorithm stem from vertical nesting, the scheme presented here can be applied as well to horizontally variable grid spacing.

Corresponding author address: Dr. Robert L. Walko, Department of Atmospheric Science, Colorado State University, Fort Collins, CO 80523.

Recent work by Skamarock and Klemp (1993) describes a nesting technique called adaptive mesh refinement, which they demonstrated in a number of simulations, including a two-dimensional collapsing cold pool. Their method of exchanging information between grids is similar to the CFCH scheme, although exact conservation of scalars and momentum (described below) is not ensured in the nesting algorithms. Numerical tests performed by Clark and Farley (1984) demonstrated superior results when conservation was followed, although in results obtained by Skamarock and Klemp conservation was not found to improve the results. Skamarock and Klemp attributed the difference to their use of the elastic set of equations (as is used in RAMS), in contrast to the anelastic set used by Clark and Farley, although no mechanism for the contrasting behavior was given. In the present nesting scheme, we apply the conservation condition of CFCH because conservation seems to be a more desirable property of a nesting algorithm than exact second-order accuracy (which is degraded as a result of conservation), and the conservation condition adds no computational expense.

Two versatile features of the nesting algorithm used by Skamarock and Klemp are 1) automatic configuring of nested grids at locations and times where higher resolution of flow features is required and 2) the freedom for a nested grid to be rotated out of alignment with the mesh of the parent grid, so that it can be aligned with a selected flow feature. Neither of these features has been implemented here, although in principle automation is fully compatible with the present scheme. Grid rotation is not possible partly because, as explained by Skamarock and Klemp, this prevents conservation without use of a complicated numerical algorithm. However, a substitute for rotation is possible

in which meshes are aligned, but the fine-mesh lateral boundaries follow general diagonal directions by stepping alternately along the orthogonal directions of the coarse-mesh grid cell boundaries. Implementation of this feature is planned in the present scheme.

2. Derivation

We shall refer to a three-dimensional computational domain with spatial coordinates (x, y, z), prognostic velocity components (u, v, w), and prognostic scalar variables s. Coordinate locations (X, Y, Z) and variables (U, V, W) and S are denoted by uppercase letters on the PG and lowercase on the NG. Velocity components are assumed to be multiplied by density, such that they actually represent momentum components. Temperature and moisture scalars represented by s and S are also density weighted, but pressure is not. As described in CFCH (refer to Fig. 1 in either paper), the grid nesting scheme is built around the Arakawa type-C grid stagger. A two-way communication of all prognostic variables is carried out between the PG and NG. Communication from the PG to the NG is accomplished following the updating of PG variables each time step. The updated variables are spatially interpolated to the NG boundaries and become the boundary values used by the NG. Interpolation of a PG variable is first carried out in the x direction in order to define the variable at the same x coordinates as the corresponding NG variable but still at the same y and z coordinates as the PG variables. A second-stage interpolation in the y direction then defines the variable at the NG x- and y-coordinate positions but at the PG z-coordinate positions. A final third-stage interpolation in the z direction completes the interpolation of the PG variables to the NG locations. The NG is then stepped forward in time until reaching the simulation time of the PG. Communication from the NG to the PG is then carried out by averaging the prognostic variables over each set of NG cells that occupy a single PG cell and replacing the PG cell value with that average. In the case of velocity components, some NG values are defined at the same x-, y-, or z-coordinate locations as the PG values; in such cases, interpolation and averaging are performed only in the other two directions. Here we will present the modifications required to the third-stage (vertical) interpolation operator and to the vertical part of the averaging operator to accommodate variable vertical grid spacing. If variable spacing were used in the horizontal directions, the same modifications would be applied there.

The derivation of the generalized nesting scheme is straightforward. It begins from the Lagrange formula for an interpolating polynomial (Abramowitz and Stegun 1965, p. 878) of which uniform spacing between points used by CFCH is a special case. Consider the diagram in Fig. 1, which depicts an x–z cross section through a portion of the computational mesh. Four

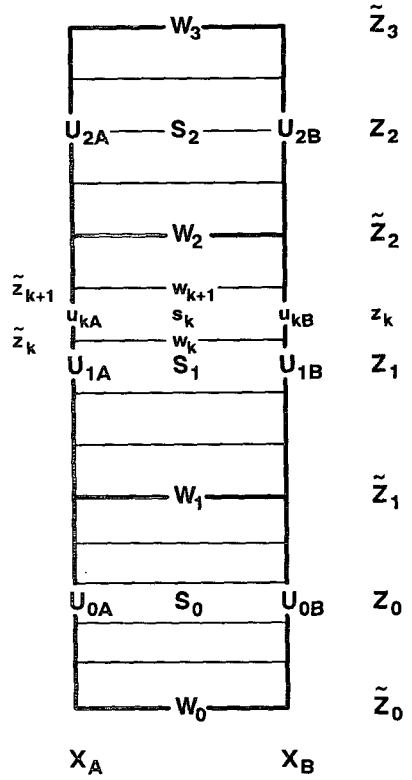

FIG. 1. A portion of the computational grid depicting three PG cells (heavy lines) inside each of which are four or five NG cells (thin lines). Variable names and coordinates denoted with uppercase letters for the PG and lowercase for the NG. A tilde is used to denote vertical coordinates at the levels of W or w points.

consecutive nonuniformly spaced W levels and the intervening grid cells of the PG are shown and labeled with arbitrary indices 0–3. Each of these cells has nested vertically within it four or five NG cells. The PG values for U, W, and S are assumed to have already been interpolated in the x and y directions and are now ready for vertical interpolation to the NG grid locations; thus, the derivation is essentially a one-dimensional scheme. The symbols A and B denote two adjacent locations in the x direction of U (and u) values. Vertical index k is used to represent an arbitrary level within the NG. As described in CFCH, spatial interpolations are quadratic (except for any velocity component interpolated in its own spatial direction) but are corrected to maintain conservation of a variable between grids. The second-order Lagrangian interpolating polynomial for s_k at any location z_k within the center PG cell is given by

$$s_k = \frac{z_k - Z_1}{Z_0 - Z_1}\frac{z_k - Z_2}{Z_0 - Z_2} S_0 + \frac{z_k - Z_0}{Z_1 - Z_0}\frac{z_k - Z_2}{Z_1 - Z_2} S_1 + \frac{z_k - Z_0}{Z_2 - Z_0}\frac{z_k - Z_1}{Z_2 - Z_1} S_2. \quad (1)$$

The vertical part of the averaging operator applied to s_k values to communicate them to the PG is

$$(\tilde{Z}_2 - \tilde{Z}_1)\bar{S} = \sum_{m=1}^{N} (\tilde{z}_{m+1} - \tilde{z}_m)s_m, \qquad (2)$$

where N is the total number of s_k values contained within the center PG cell (five in the example of Fig. 1) and $\bar{S}$ is the resulting average that will replace S_1. Weighting the s_m values by the corresponding thickness $z_{m+1} - z_m$ of each NG cell, and $\bar{S}$ by the thickness $\tilde{Z}_2 - \tilde{Z}_1$ of the PG cell, makes the volume integral of s and S conservative between grids. Since the scalars (and velocities) are density weighted, this implies conservation of thermal energy, mass, and momentum. The scheme of CFCH also requires conservation of the volume integrals of s and S in the application of Eq. (1); that is, all N values of s_k obtained by Eq. (1) must satisfy Eq. (2) with $\bar{S}$ replaced by S_1. This is equivalent to a reversibility condition in which application of Eq. (1) to obtain all s_k values, followed by application of Eq. (2) using these s_k values, gives a value of $\bar{S}$ that is identical to S_1. In general, this condition is not satisfied, so Eq. (1) is modified by adding a constant C to its right-hand side. This causes all s_k values in the center PG cell to be changed by the same amount C, which is equivalent to most closely matching the original interpolating polynomial in a least-squares sense (CFCH). We find the expression for C by setting $\bar{S}$ equal to S_1 in Eq. (2) and by substituting the modified Eq. (1) for each s_m in the summation in Eq. (2), obtaining the expression

$$C = S_1 - \frac{1}{\tilde{Z}_2 - \tilde{Z}_1} \sum_{m=1}^{N} (\tilde{z}_{m+1} - \tilde{z}_m) \times \left(\frac{z_m - Z_1}{Z_0 - Z_1}\frac{z_m - Z_2}{Z_0 - Z_2} S_0 + \frac{z_m - Z_0}{Z_1 - Z_0}\frac{z_m - Z_2}{Z_1 - Z_2} S_1 + \frac{z_m - Z_0}{Z_2 - Z_0}\frac{z_m - Z_1}{Z_2 - Z_1} S_2 \right). \qquad (3)$$

Substituting this expression in Eq. (1) gives

$$s_k = D_0 S_0 + D_1 S_1 + D_2 S_2, \qquad (4)$$

where

$$D_0 = \frac{z_k - Z_1}{Z_0 - Z_1}\frac{z_k - Z_2}{Z_0 - Z_2} - \frac{1}{\tilde{Z}_2 - \tilde{Z}_1} \times \sum_{m=1}^{N} (\tilde{z}_{m+1} - \tilde{z}_m)\left(\frac{z_k - Z_1}{Z_0 - Z_1}\frac{z_k - Z_2}{Z_0 - Z_2} \right),$$

$$D_1 = \frac{z_k - Z_0}{Z_1 - Z_0}\frac{z_k - Z_2}{Z_1 - Z_2} + 1 - \frac{1}{\tilde{Z}_2 - \tilde{Z}_1} \times \sum_{m=1}^{N} (\tilde{z}_{m+1} - \tilde{z}_m)\left(\frac{z_k - Z_0}{Z_1 - Z_0}\frac{z_k - Z_2}{Z_1 - Z_2} \right),$$

$$D_2 = \frac{z_k - Z_0}{Z_2 - Z_0}\frac{z_k - Z_1}{Z_2 - Z_1} - \frac{1}{\tilde{Z}_2 - \tilde{Z}_1} \times \sum_{m=1}^{N} (\tilde{z}_{m+1} - \tilde{z}_m)\left(\frac{z_k - Z_0}{Z_2 - Z_0}\frac{z_k - Z_1}{Z_2 - Z_1} \right).$$

The coefficients D_0, D_1, and D_2 are all constant in time, being a function only of the vertical coordinates of the PG and NG levels, and can be precomputed. The scheme is thus as computationally efficient as on a grid of constant spacing. Under the condition of constant grid spacing, the coefficients reduce to Eqs. (33) and (36) in Clark and Farley (1984).

Equations (2) and (4) apply also to the horizontal velocity components by substituting U and u, or V and v, for S and s. For u at X_A and X_B, this is written

$$u_{kA} = D_0 U_{0A} + D_1 U_{1A} + D_2 U_{2A}, \qquad (5)$$

$$u_{kB} = D_0 U_{0B} + D_1 U_{1B} + D_2 U_{2B}. \qquad (6)$$

The NG w values, however, require a more complicated interpolating formula. We first note that some w values coincide with the W values (after the latter have been interpolated in the x and y directions). In these cases, no vertical interpolation is performed, but W directly replaces w. We note also (CFCH) that no vertical averaging of w is required to obtain W; only horizontal averaging is performed. However, w values at levels between those where W values are defined do require vertical interpolation from the PG.

Derivation of the interpolation formula is based on the requirement of three-dimensional mass continuity and thus makes reference to horizontal velocity components. As will be shown, however, the formula reduces to a function of W values only. For simplicity, we consider motions only in the x–z plane, but inclusion of the V and v components of motion is straightforward. Referring again to Fig. 1, the conditions for mass continuity on the PG and NG are

$$(U_{jB} - U_{jA})(\tilde{Z}_{j+1} - \tilde{Z}_j) + (W_{j+1} - W_j)(X_B - X_A) = 0, \qquad (7)$$

$$(u_{kB} - u_{kA})(\tilde{z}_{k+1} - \tilde{z}_k) + (w_{k+1} - w_k)(X_B - X_A) = 0, \qquad (8)$$

for any j and k. Using the interpolation formulas in Eqs. (5) and (6), we express u_{kB} and u_{kA} in Eq. (8) in terms of U on the PG. This leads to terms of the form $U_{jB} - U_{jA}$, which we replace by expressions in W using Eq. (7). This gives

$$\frac{w_{k+1} - w_k}{\tilde{z}_{k+1} - \tilde{z}_k} = D_0 \frac{W_1 - W_0}{\tilde{Z}_1 - \tilde{Z}_0} + D_1 \frac{W_2 - W_1}{\tilde{Z}_2 - \tilde{Z}_1} + D_2 \frac{W_3 - W_2}{\tilde{Z}_3 - \tilde{Z}_2}. \qquad (9)$$

Rearrangement of Eq. (9) leads to

$$w_{k+1} = w_k + [-E_{0k}W_0 + (E_{0k} - E_{1k})W_1 + (E_{1k} - E_{2k})W_2 + E_{2k}W_3], \qquad (10)$$

where

$$E_{jk} = \frac{D_j(\tilde{z}_{k+1} - \tilde{z}_k)}{\tilde{Z}_{j+1} - \tilde{Z}_j}.$$

Equation (10) is a recursion relation that is easily evaluated for all w_k values not collocated with W values, starting from those that are collocated and therefore replaced by direct assignment from horizontally interpolated W. Since the coefficients E_{jk} are all constant in time, they can be precomputed, making evaluation of Eq. (10) very efficient during model run time.

3. Other considerations

We mention here a few miscellaneous aspects of the generalized nesting scheme.

1) As in Clark and Hall (1991) and Skamarock and Klemp (1993), temporal refinement is used with grid nesting. Parent grid values that are interpolated spatially to the NG boundaries are also interpolated linearly in time between consecutive PG time steps to define them at intermediate NG time steps.

2) Over elevated terrain, all vertical coordinates referred to in this paper are actually terrain-following sigma–z coordinates (Gal-Chen and Somerville 1975). No modifications to the nesting scheme are required for the transformed coordinates because the transformation over elevated terrain causes a vertical compression of vertical levels where the compression ratio is constant with height, varying only with horizontal position. All the geometric coefficients in Eqs. (2), (4), and (10) are (or can be written in terms of) dimensionless quotients of vertical distances and are thus unchanged.

3) Discrete horizontal movement of nested grids is allowed in RAMS and is useful for following a structure requiring enhanced resolution such as a convective cell or a tropical cyclone. Each discrete movement of a grid is a displacement over a distance of one mesh cell on the parent grid. The field variables are adjusted over most of the displaced grid by shifting them on the grid so that specific values have the same absolute (geographic) location as before the mesh moved. Along the leading edge of the moved grid, and inward for a distance of one parent grid-mesh cell, the field variables are redefined on the nested grid by interpolation from the parent grid, since high resolution fine grid values did not exist at that absolute location before the displacement. This interpolation, and also the initial interpolation of variables onto the entire fine grid at the beginning of a simulation, are performed using Eq. (4). Moving grids present no special problems for the generalized nesting scheme. The weighting coefficients in Eqs. (2), (4), and (10) are independent of horizontal grid position and do not require recomputation each time the grid moves.

4) In using variable vertical grid spacing to increase resolution near the ground, it is preferable to avoid large expansion ratios $\tilde{R}_j$ between consecutive levels, where $\tilde{R}_j$ is defined for any level j as

$$\tilde{R}_j \equiv \frac{(\Delta\tilde{Z})_j}{(\Delta\tilde{Z})_{j-1}}, \tag{11}$$

and

$$(\Delta\tilde{Z})_j \equiv \tilde{Z}_{j+1} - \tilde{Z}_j, \tag{12}$$

using the notation in Fig. 1. We thus usually employ a fairly small fixed value of $\tilde{R}_j$ over many levels such that the grid varies geometrically from small $\Delta\tilde{Z}_j$ values near the ground to much larger ones aloft. For example, with $\tilde{R}_j = 1.15$, $(\Delta\tilde{Z})_j$ increases tenfold in about 16 levels. Often, we impose an upper bound on $(\Delta\tilde{Z})_j$, which leads to $\tilde{R}_j = 1$ when the bound is reached. We also desire that NG levels be stretched geometrically when those on the PG are. Since it is not always required that $\tilde{R}_j$ be constant, we define an average PG stretch ratio R_j for the grid cell between $\tilde{Z}_{j+1}$ and $\tilde{Z}_j$ as

$$R_j = \left[\frac{(\Delta\tilde{Z})_{j+1}}{(\Delta\tilde{Z})_{j-1}}\right]^{0.5}, \tag{13}$$

which is the geometric mean of $\tilde{R}_{j+1}$ and $\tilde{R}_j$. The appropriate constant stretch ratio $\tilde{r}_k$ applied to all N NG cells inside this PG cell is

$$\tilde{r}_k = (R_j)^{1/N}, \tag{14}$$

where

$$\tilde{r}_k \equiv \frac{(\Delta\tilde{z})_k}{(\Delta\tilde{z})_{k-1}}, \tag{15}$$

and

$$(\Delta\tilde{z})_k \equiv \tilde{z}_{k+1} - \tilde{z}_k. \tag{16}$$

This relation, coupled with the requirement

$$\sum_{k=1}^{N} (\Delta\tilde{z})_k = (\Delta\tilde{Z})_j \tag{17}$$

determines all levels $\tilde{z}_k$. In cases where $\tilde{R}_j$ is constant with height, this formulation causes $\tilde{r}_k$ to also be constant, even between PG cells. Similarly, we make distances between $\tilde{Z}$ and Z levels (and $\tilde{z}$ and z levels) expand geometrically by setting

$$\frac{\tilde{Z}_{j+1} - Z_j}{Z_j - \tilde{Z}_j} = (R_j)^{0.5}, \tag{18}$$

and

$$\frac{\tilde{z}_{k+1} - z_k}{z_k - \tilde{z}_k} = (r_k)^{0.5}. \tag{19}$$

5) Each time the vertical nesting ratio changes with height, such as the jump from 4 to 5 shown in Fig. 1,

the vertical grid spacing on either the NG, the PG, or both must also make a jump. This is especially true when the nest ratio changes from 1 to 2. It is desirable to keep the maximum grid spacing jump ratio as small as possible, and this can be accomplished by sharing the jump between the PG and NG. In the example of Fig. 1, the PG spacing $\tilde{Z}_3 - \tilde{Z}_2$ would be made slightly less than $\tilde{Z}_2 - \tilde{Z}_1$ so that the lowest NG cell in the upper PG cell is not too much larger than the highest NG cell in the middle PG cell. Since the PG spacing usually increases with height, this would involve a local disruption of the increase.

6) It is not required that an NG start from the ground or extend to the top of the PG. If it does, however, the interpolating formula Eq. (10) references a W and $\tilde{Z}$ value (for either case), which is beyond the spatial boundary of the PG and is not defined. The missing W values are computed using Eq. (7) with the V component included, and the missing $\tilde{Z}$ value is computed from Eqs. (11) and (12) by assuming that $\tilde{R}_i$ is constant with height at either boundary. If an NG extends to the top and bottom of the PG, Eqs. (4) and (10) are applied to the top and bottom boundaries and to the interior of the NG only when it is initialized; in subsequent time steps, Eqs. (4) and (10) are applied only at the lateral boundaries of the NG. For a top and/or bottom face of the NG contained within the interior of the PG, Eq. (4) is applied at each time step. However, Eq. (10) is not required because the NG top and bottom boundary values of w are at the same levels as W values on the PG and thus require only horizontal interpolation.

One issue that arises when an NG does not extend as high as the PG is that electromagnetic radiative fluxes must be communicated between grids through the top NG boundary. Not only does the NG require information such as cloudiness from the PG levels above it, but those PG levels should in turn receive information from the NG rather than the PG levels below. For example, an NG may contain partial, small-scale cloud cover, causing radiative absorption and emission over a fraction of its horizontal area. Application of Eq. (2) to the NG moisture field could lead to no cloudiness or to complete cloud cover on the PG because of its inability to resolve the NG clouds. Clearly,

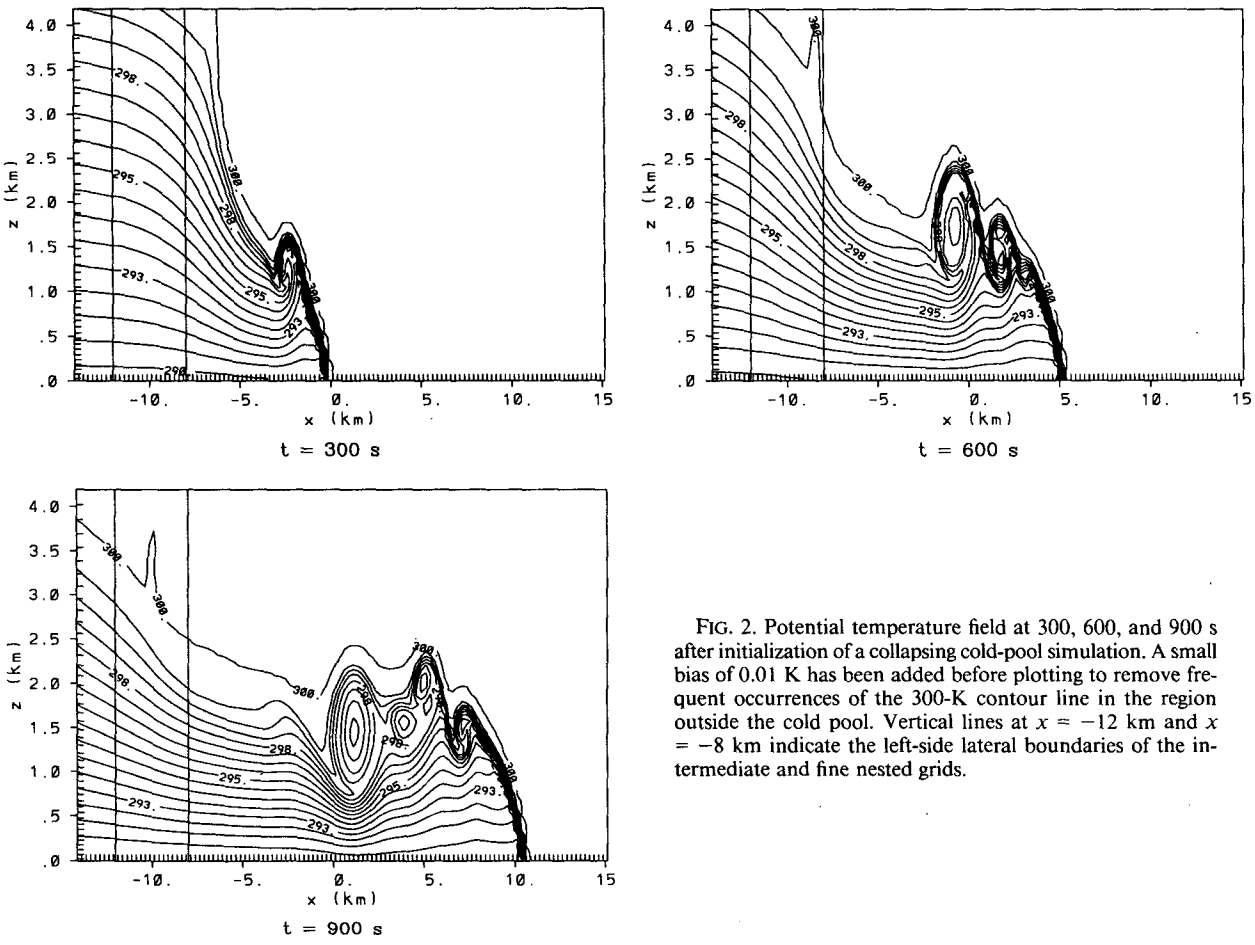

FIG. 2. Potential temperature field at 300, 600, and 900 s after initialization of a collapsing cold-pool simulation. A small bias of 0.01 K has been added before plotting to remove frequent occurrences of the 300-K contour line in the region outside the cold pool. Vertical lines at $x = -12$ km and $x = -8$ km indicate the left-side lateral boundaries of the intermediate and fine nested grids.

the NG cloud field provides a more accurate representation of radiative transfer. A new RAMS radiation parameterization, which will include nesting communication of radiative fluxes, is under development.

4. Numerical test

We demonstrate the performance of the generalized nesting scheme in RAMS for a simulation of a collapsing cold pool, as in Skamarock and Klemp (1993). A two-dimensional model domain 10 km deep and 40 km long is used with the constraint of zero horizontal velocity imposed at the left end of the domain ($x = -20$ km). The initial state is motionless and has a potential temperature given by

$$\theta = \begin{cases} 300 - \left(\dfrac{5000 - z}{500}\right), & \text{for} \quad z \leqslant 5000 \text{ m}; \\ \quad x \leqslant -5000 \text{ m} \\ 300, \quad \text{elsewhere.} \end{cases} \tag{20}$$

Three levels of grid nesting are used, with horizontal mesh sizes of 250, 83.3, and 27.8 m as in Skamarock and Klemp. Our meshes are stretched in the vertical, thus differing from theirs. The vertical grid spacing on the coarse and intermediate meshes is 50 m at the ground and is stretched geometrically at 3% per level, reaching a spacing of about 450 m at the model top using 68 levels. The fine mesh incorporates 5 vertical levels within each level of the intermediate grid up to a height of 3 km. This nesting ratio is reduced to 4:1 over the next 5 intermediate grid levels, 3:1 over the next 5, and 2:1 over the next 5, finally maintaining 1:1 above. This results in a fine grid vertical spacing of 10 m at the ground and 27 m at a height of 3 km. The intermediate grid covers the domain between $x = -12$ km and $x = 17$ km, while the fine grid extends from $x = -8$ km to $x = 14$ km. A turbulent mixing coefficient of 27.8 m^2 s^{-1} is used on all grids. Conditions of free slip and zero heat flux are used at the lower boundary. In the absence of surface drag, there is little need for high vertical resolution near the ground, but stretching is used nevertheless to demonstrate its compatibility with the generalized nesting algorithm.

Results of this simulation are shown in Fig. 2 at times 300, 600, and 900 s after initialization and may be compared with Figs. 4b and 5 in Skamarock and Klemp (1993), noting that the x coordinate in the current case is offset by 20 km. We have positioned the fine grid so that the sharp gradient regions of the wave front remain within it for the entire simulation since, as demonstrated in Fig. 4a of Skamarock and Klemp, the coarser resolution does not adequately resolve the high-gradient region. However, disturbances of weaker gradient travel upstream from the initial wavefront at $x = -5$ km, passing through both nested grid boundaries, and show no evidence of the boundaries. These results indicate that momentum fluxes and potential temperatures are successfully communicated between grids.

5. Conclusions

We have described a generalization to an existing computational grid nesting algorithm that extends its applicability to stretched grids and spatially variable nesting ratios. The usual condition that an integer number of fine mesh cells exactly occupy a single coarse-mesh cell is followed in this algorithm. The scheme has been applied in the vertical to provide increased vertical resolution on selected levels within a nested grid but can be applied as well to the horizontal directions. The scheme was demonstrated in a simulation of a collapsing cold pool with good results.

Acknowledgments. This work was supported under NSF Grants ATM 8915265 and ATM 9118963, and by ASTeR, Inc. We thank Joseph Klemp for an informative review that improved the paper. Tony Smith helped in the preparation of the manuscript.

REFERENCES

Abramowitz, M., and I. A. Stegun, 1965: *Handbook of Mathematical Functions.* National Bureau of Standards, Applied Mathematics Series 55, U.S. Department of Commerce, Washington, DC, 1046 pp.

Clark, T. L., and R. D. Farley, 1984: Severe downslope windstorm calculations in two and three spatial dimensions using anelastic interactive grid nesting: A possible mechanism for gustiness. *J. Atmos. Sci.*, **41**, 329–350.

——, and W. D. Hall, 1991: Multi-domain simulations of the time dependent Navier–Stokes equations: Benchmark error analysis of some nesting procedures. *J. Comput. Phys.*, **92**, 456–481.

Gal-Chen, T., and R. C. J. Somerville, 1975: On the use of a coordinate transformation for the solution of the Navier–Stokes equations. *J. Comput. Phys.*, **17**, 209–228.

Skamarock, W. C., and J. B. Klemp, 1993: Adaptive grid refinement for two-dimensional and three-dimensional nonhydrostatic atmospheric flow. *Mon. Wea. Rev.*, **121**, 788–804.